Organic & Biomolecular Chemistry

Cite this: *Org. Biomol. Chem.*, 2011, **9**, 4234

www.rsc.org/obc

PAPER

C-hexaphenyl-substituted trianglamine as a chiral solvating agent for carboxylic acids†

Andrea Gualandi,*[a] Stefano Grilli,[a] Diego Savoia,[a] Marcin Kwit[b] and Jacek Gawroński*[b]

Received 16th December 2010, Accepted 17th March 2011
DOI: 10.1039/c0ob01192d

Chiral hexaazamacrocycles with a trianglamine structure and C_3-symmetry, containing six ring substituents and twelve stereocenters have been tested as chiral solvating agents (CSAs) for α-substituted carboxylic acids. Excellent results have been obtained with a hexaphenyl-substituted macrocycle. The optimal ratio between the macrocycle and racemic acid, allowing for baseline separation of the enantiomers' signals in the ^{1}H NMR spectrum, was dependent on the type of acid, in particular on its degree of acidity. The analyte and the CSA could be separated and recovered by a simple acid–base extraction and reused without purification. The conformations of the free and protonated hexaamino macrocycles were inferred by CD spectroscopic studies and DFT calculations.

Introduction

The increasing demand for enantiomerically pure compounds from academics and industry has stimulated the development of efficient strategies for their synthesis and fast and accurate analytical methods for the determination of their enantiomeric excess.[1] Chromatographic[2] and spectroscopy methods[3] are useful for meeting this demand.[4] In particular, NMR spectroscopy is easy, fast and it could be considered an environmentally friendly technique because only small amounts of deuterated solvent, a few milligrams of product and a common NMR spectrometer are required for the analysis. However, a chiral additive is required to modify the environment from achiral to chiral and make it possible to distinguish between the two enantiomers of the analyte. The chiral additive converts the mixture of enantiomers in a mixture of diasteromeric species in two different ways: (a) by forming a covalent bond with the analyte, and in this case the additive is a "chiral derivatizing agent" (CDA);[5] (b) by forming a labile supramolecular interaction, so it acts as a "chiral solvating agent" (CSA). The use of CDAs can involve kinetic resolution of the substrate and requires purification of the sample, whereas CSAs do not present such disadvantages and the sample can be easily recovered after the analysis.

Different CSAs have been developed in the last few years, *e.g.* pincer-like diamines,[6] alkaloids,[7] BINOL derivatives,[8] porphyrins,[9] cyclodextrins,[10] and macrocycles.[11] Among the latter compounds, chiral perazamacrocycles[12] derived from enantiomerically pure *trans*-1,2-diaminocyclohexane have been employed.[13–16] Tanaka and co-workers[15] reported the use of trianglamine **1a**[16] (Fig. 1) as a useful CSA for secondary alcohols, cyanohydrins and propargylic alcohols, but unsuccessful results were obtained with the same receptor for carboxylic acids. Better results for the determination of the optical purity of carboxylic acids were instead obtained using host **2**,[17] where the presence of phenolic hydrogen bond donors increased the number of binding sites for the guest molecules.

Members of our group have recently reported the diasteroselective synthesis of trianglamines **1b** and **c** (Fig. 1) by the addition of organolithium reagents to the trianglimine derived from (*R*,*R*)-1,2-diaminocyclohexane and terephthalaldehyde with complete stereocontrol giving the *R* configuration of all six newly formed stereocenters.[18] Hence, based on the previously reported failure of **1a** to act as an effective receptor of carboxylic acids,[15] we began to investigate the application of the C-hexaphenyl-substituted trianglamine **1c** for the same purpose. The macrocycle **1b** was not considered for the enantiodiscrimination experiment due to the multiplicity of its ^{1}H NMR signals.

When the work presented herein was almost complete, we became aware of a recent paper by Periasamy,[19] who described the use of diamines and macrocyclic polyamines derived from (*R*,*R*)-1,2-diaminocyclohexane for the enantiodiscrimination of carboxylic acids. In particular, it was shown that **1a** is an efficient CSA for mandelic acid, in contrast to the failure reported by Tanaka.[15]

Herein, we describe the results of the thorough study of the receptor capability of **1c** towards a variety of α-chiral carboxylic acids by the usual NMR methods, together with relative CD spectroscopic studies and DFT calculations.

[a]*Dipartimento di Chimica "G. Ciamician", Alma Mater Studiorum Università di Bologna, via Selmi 2, 40126, Bologna, Italy. E-mail: andrea.gualandi10@unibo.it*
[b]*Department of Chemistry, Adam Mickiewicz University, 60-780, Poznań, Poland. E-mail: gawronsk@amu.edu.pl*

† Electronic supplementary information (ESI) available: NMR spectra, calculated ECD and UV spectra, relative energies, percentage populations and values of torsion angles calculated for **1b** and **1c**. See DOI: 10.1039/c0ob01192d

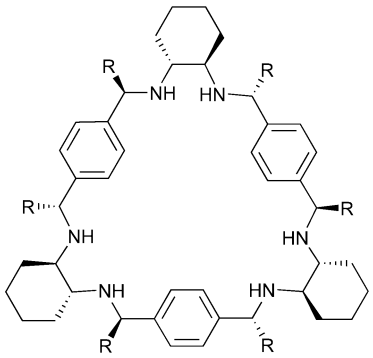

1a: R = H
1b: R = Me
1c: R = Ph

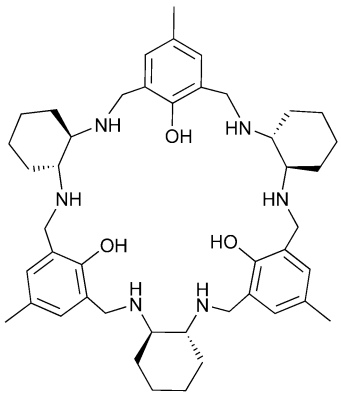

2

Fig. 1 Chiral perazamacrocyclic CSA.

Results and discussion

^{1}H NMR enantiodiscrimination experiments

The experiments were performed by adding increasing amounts of racemic carboxylic acids **3–6** to a solution of **1c** (10 mM in $CDCl_3$) in an NMR tube. Immediately after each addition, the ^{1}H NMR spectrum was acquired at 400 MHz at 25 °C. Table 1 shows the values of the induced chemical shifts ($\Delta\delta$) on selected signals of *rac*-carboxylic acids **3–6** (Fig. 2) and the difference between the signal corresponding to each enantiomer of the acid ($\Delta\Delta\delta$) after the addition of **1c**, in the optimal ratio to observe the baseline separation of the signals of the two enantiomers.

As a general trend, the average signal of the protons of the two enantiomers of the acid move upfield ($\Delta\delta < 0$), suggesting deprotonation of the carboxylic function. At the same time, the absorption of the benzylic proton of the macrocycle **1c** moved downfield ($\Delta\delta > 0$), which indicated that an acid–base reaction occurred between the two species. Increasing the amount of acid meant the ^{1}H NMR benzylic signal of **1c** kept moving downfield, while the signal of the acid kept moving upfield, approaching the position of the signal observed for a solution of the acid.

The first acid to be studied was mandelic acid. After the addition of 0.5 equivalent of racemic mandelic acid **3a** to a solution of **1c** (Fig. 3), the chemical shift values of the $C_\alpha H$ proton of the two enantiomers were split by 0.033 ppm, and the addition of an excess of (*R*)-**3a** allowed attribution of the singlet at higher field to (*R*)-**3a**. The difference between the chemical shifts of the enantiomers ($\Delta\Delta\delta$) increased gradually up to 0.044 ppm when 10 equiv. **3a** were added. Then further addition of **3a** caused a continuous decrease of $\Delta\Delta\delta$ down to 0.030 ppm when 20 equiv. **3a** were added. It is noteworthy that the signals relative to $C_\alpha H$ of (*R*)-**3a** and the benzylic proton of **1c** were broadened by increasing the amount of **3a** added. It is noteworthy that all of the ^{13}C NMR signals relative to the two enantiomers of **3a** in the presence of 0.5 equiv. of **1c** were split.[20]

A comparison with the outcome of an analogous experiment was carried out with the unsubstituted macrocyclic receptor **1a**. In this case, maximum splitting (0.044 ppm) of the $C_\alpha H$ signal occurred when 3 equivalents of mandelic acid **3a** were added to **1a**. Hence, to achieve the same splitting, a minor amount of **1c** is necessary compared to the amount of **1a**.

Analogous behaviour was observed for racemic α-chlorophenylacetic acid **3b**, but in this case, the signal relative to $C_\alpha H$ of the two enantiomers overlapped the benzylic signal of **1c** until 4 equiv. of **3b** were added. After that, the baseline separation

Table 1 Measurement of the induced chemical shifts ($\Delta\delta$) and chemical shift non-equivalences ($\Delta\Delta\delta$) of selected probe signals for a mixture of **1c** and different guests with ^{1}H NMR (400 MHz, 10 mM in $CDCl_3$, 25 °C)

Acid	**1c** : Acid ratio	Probe signal	$\Delta\delta^a$ (ppm)	$\Delta\Delta\delta$ (ppm)
3a	1 : 10	$C_\alpha H$	–0.319	0.044
3b	1 : 14	$C_\alpha H$	–0.227	0.061
3c	1 : 10	$C_\alpha H$	–0.165	0.066
3d	1 : 0.5	$C_\alpha H$	–0.360	0.066
		OCH_3	–0.323	0.023
3d	1 : 4	$C_\alpha H$	–0.224	0.033
		OCH_3	–0.323	0.037
3e	1 : 0.25	$C_\alpha H$	–0.166	0.006
		CH_3	–0.168	0.119
3f	1 : 0.2	$C_\alpha H$	–0.316	0.006
		CH_3	–0.297	0.062
		$C_\alpha H$	–0.178	0.002
4	1 : 0.25	CH_2CH	–0.019	0.010
		$CHCH_3$	–0.184	0.058
		$CH(CH_3)_2$	–0.003	0.008
5	1 : 0.25	$C_\alpha H$	–0.220	0.002
		OCH_3	–0.004	0.010
		CH_3	–0.204	0.051
6	1 : 4	$COCH_3$	–0.319	0.057
		CH_3	–0.143	0.027

[a] The difference between the signals in a solution of the acid and the average of the signals of the two enantiomers after the addition of **1c**.

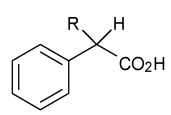

3a: R = OH
3b: R = Cl
3c: R = Br
3d: R = OMe
3e: R = OAc
3f: R = Me

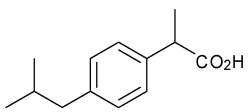

4

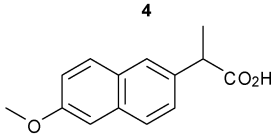

5

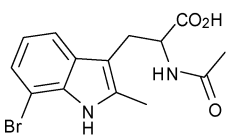

6

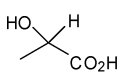

7

Fig. 2 The chiral carboxylic acids subject to study.

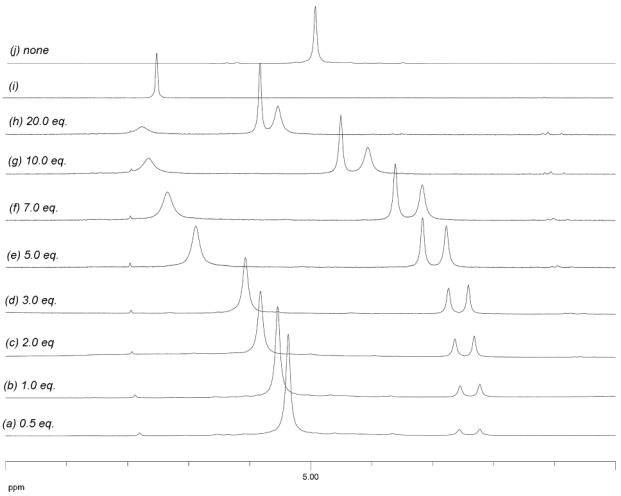

Fig. 3 Partial ^{1}H NMR spectra (400 MHz, $CDCl_3$, 25 °C) showing: (*a–h*) the $C_\alpha H$ signal of **3a** and the PhCH signal of **1c** after the addition of different aliquots of **3a** to a 10 mM solution of **1c**; (*i*) $C_\alpha H$ signal of **3a**; (*j*) PhCH signal of **1c**.

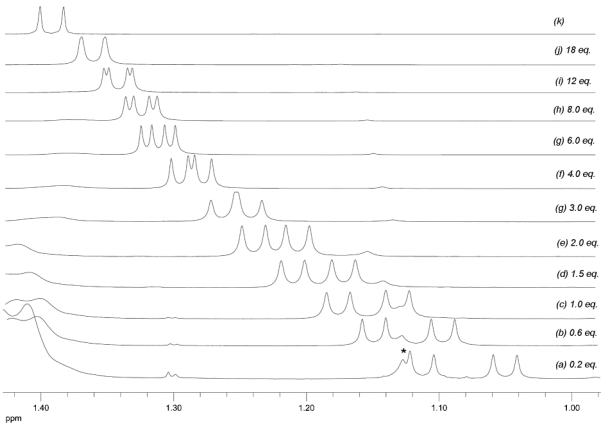

Fig. 4 (*a–j*) Partial ^{1}H NMR spectra (400 MHz, $CDCl_3$, 25 °C) of **3f** showing signals of the methyl group after the addition of aliquots of **3f** to a 10 mM solution of **1c**. (*k*) A partial ^{1}H NMR spectrum (400 MHz, 10 mM, $CDCl_3$, 25 °C) of **3f** showing the $-CH_3$ signal.

of the signals relative to the two enantiomers was observed as $\Delta\Delta\delta$ 0.042 ppm, which increased up to 0.061 ppm when 14 equiv. of **3b** were added and it remained constant after further addition of the acid. The chiral macrocycle **1c** demonstrated similar behaviour towards α-bromophenylacetic acid **3c**, for which the maximum $\Delta\Delta\delta$ value of 0.066 ppm was reached when 10 equiv. acid were added to the ligand.

On the other hand, 2-methoxyphenylacetic acid **3d** interacted with **1c** in a different way, as addition of increasing amounts of acid caused a decrease in $\Delta\Delta\delta$ for the signals relative to $C_\alpha H$, while an increase was observed for the OCH_3 signals. The maximum enantiodiscrimination was observed for $C_\alpha H$ ($\Delta\Delta\delta$ = 0.066 ppm) and for OCH_3 ($\Delta\Delta\delta$ = 0.037 ppm) when 0.5 and 4 equiv. of acid were added, respectively.

Similar behaviour was observed for 2-acetoxyphenylacetic acid (**3e**). In this case, the signals of the methyl (acetoxy) group of the two enantiomers were split by 0.119 ppm when 0.25 equiv. of **3e** were added, whereas the $C_\alpha H$ signal presented a small $\Delta\Delta\delta$ value (0.006 ppm). Unfortunately, the signal of the methyl group partially overlapped the ligand signal and these were not useful for the determination of the enantiomeric excess.

Using 2-phenylpropionic acid (**3f**), the splitting of the $C_\alpha H$ signal was smaller than the width of the quartet and overlapping of the signals was observed. However, baseline separation for the signals relative to the CH_3 group of the two enantiomers was observed until 2 equiv. of **3f** were added, after which the two signals overlapped and became unsuitable for use in enantiomeric excess determination (Fig. 4).

Then, the use of the chiral macrocycle **1c** for enantiomeric discrimination of non-steroidal anti-inflammatory drugs ibuprofen (**4**) and naproxen (**5**) was investigated. A clear separation of the CH_3 and CH_2 groups of **4** and the CH_3 and OCH_3 groups of **5** was observed when 0.25 equiv. of acid were added, whereas the $C_\alpha H$ signal showed a very small $\Delta\Delta\delta$ for both of the acids. For both **4** and **5**, the signals of choice for the determination of enantiomeric excess were those relative to the α-CH_3 group. As previously observed for **3f**, increasing the amount of acid with respect to **1c** caused reduced enantiodiscrimination.

The signals of the two enantiomers of racemic tryptophan derivate **6** could be separated and distinguished from the host signals only when 4 equiv. of **6** were added to **1c**. In particular, the signals of the methyl substituent in the indole ring and the acetyl group were split by 0.027 ppm and 0.057 ppm, respectively. Other signals were present as multiplets and/or were not separated from the signals of **1c**. The test using racemic lactic acid **7** provided unsuccessful results and no separation of the signal of the two enantiomers was observed. These results demonstrate that an aromatic moiety has to be present in the carboxylic acid in order to obtain a good value of enantiodiscrimination.

The stoichiometry of the most stable complex formed between **1c** and **3a** was determined according to the Job's method of continuous variation.[21] Different ^{1}H NMR spectra (400 MHz, $CDCl_3$, 25 °C) of mixtures of different ratios of **1c** with (*R*)- or (*S*)-**3a** at a constant total concentration of 10 mM were recorded and the complexation induced shift ($\Delta\delta$) of the benzylic signal of **3a** multiplied by the molar fraction of (*R*)- or (*S*)-**3a** (X**3a**) was plotted *vs*. X**3a** itself (Fig. 5). A maximum was observed when the ratio between **1c** and (*R*)- or (*S*)-**3a** was 1 : 2.33 (X**3a** = 0.7), which indicated that **1c** forms the most stable complex with two

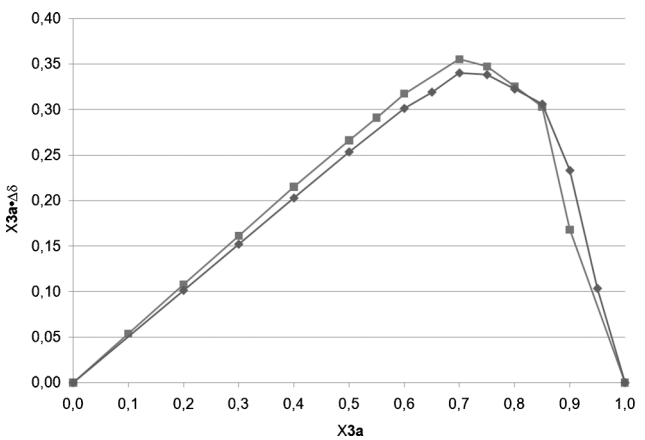

Fig. 5 Job's plots for interaction of **1c** with (*R*)-**3a** (◆) and (*S*)-**3a** (■).

molecules of **3a**. However, the presence of a multimolecular system in solution avoided the easy determination of the association constant of the substrate with **1c**.

A correlation between the enantiodiscrimination ($\Delta\Delta\delta$) and the host/guest ratio was obtained considering the acidity of the carboxylic acid, as suggested by Zhang.[22] Upon increasing the strength of the acid, lower host : guest ratios were required to have the optimal separation of the two signals relative to the enantiomers of the acid. This could be explained by the fact that weaker acids (*e.g.* **3f**) form a salt with **1c** through partial proton transfer, whereas stronger acids (*e.g.* **3a**) gave complete proton transfer in a non-polar solvent. When further amounts of a strong acid were added to hexaamine **1c**, multiprotonated species were completely formed and no residual free acid remained in solution, and thus the $\Delta\Delta\delta$ increased. On the other hand, increasing the amount of a weak acid with respect to **1c** resulted in an incremental increase in the amount of free acid, and thus the $\Delta\Delta\delta$ decreased.

A bidimensional ROE (Rotating–frame Overhauser Enhancement Spectroscopy) NMR experiment conducted on a solution of macrocycle **1c** with a two-fold excess of racemic mandelic acid **3a** showed no spatial correlation between the two species.[20] Contrastingly, selective 1D-ROESY experiments conducted on both 1 : 2 mixtures of **1c** each with a single enantiomer of mandelic acid **3a** (Fig. 6), obtained by selective irradiation at the absorption frequency of the corresponding $C_\alpha H$, displayed a positive, though small, enhancement of the phenylene protons of the macrocycle (7.39 ppm), proving that the mandelic acid is spatially close enough to the macrocycle. Assuming the ROE enhancement of mandelic *meta*-protons (7.13–7.20 ppm) identical for both the enantiomers of **3a**, a different ROE response resulted for the other aromatic signals with the two enantiomers, meaning different spatial disposition of them within the macrocycle. Particularly, relative ROE enhancement on the phenylene protons was greater for the complex **1c**–(*R*)-**3a**, so proving that there is a shorter distance between the two species with respect to the other complex. Due to the overlapping of the *ortho*-CH signals of **3a** and the substituent phenyl rings of **1c**, it was not possible to quantify the relative ROE for each of them. These experimental results pointed out that each enantiomer of **3a** included in the complex is subject to a different magnetic environment, which is supported by the non-equivalent chemical shifts of the corresponding $C_\alpha H$ protons.

Finally, to prove the accuracy of the method for the determination of the e.e. of carboxylic acids using **1c** as a CSA, samples of mandelic acid (**3a**) of different enantiopurities were prepared and their ^1H NMR spectra in $CDCl_3$ solution were recorded in the presence of **1c** (Fig. 7). The high linear correlation ($R^2 = 0.9994$) between the theoretical and observed e.e. demonstrated the applicability of the macrocyclic compound **1c** for the determination of the enantiopurity of carboxylic acids.

Computational studies

These studies raised a question regarding the effect of C-phenyl or C-methyl substitution on the enantiodiscrimination of acids and the effect, if any, of protonation of the nitrogen atoms on the conformation of the trianglamines. In fact, trianglamines **1** represent a class of heteraphanes of considerable conformational freedom, due to their low rotational barriers around the numerous single bonds. Recently members of our group reported on the conformational and chiroptical properties of the simplest trianglamine, **1a**.[16]

In the present study, we combined experimental ECD measurements with MM/DFT calculations of the structures of the possible conformers of **1b**, **1c** and **1c** × $6H^+$ and calculations of the rotational strengths of low-energy conformers. Computational analyses were performed as follows: (i) generation of the possible

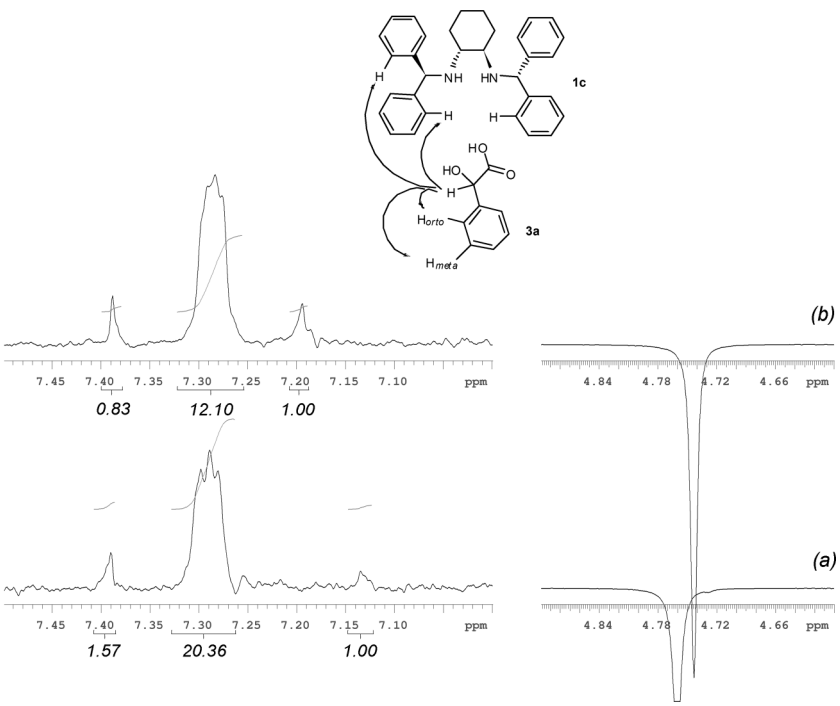

Fig. 6 Partial 1D-ROESY (400 MHz, $CDCl_3$, mixing time 0.6 s, 25 °C) spectra of a 1 : 2 mixture of **1c** with: (a) (*R*)-**3a**; (b) (*S*)-**3a**.

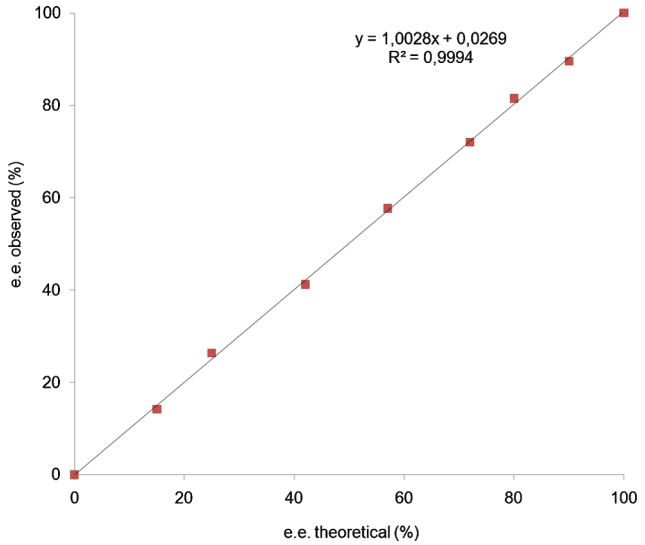

Fig. 7 The correlation between the theoretical and observed e.e. values of different solutions of **3a** (10 mM) in the presence of 0.1 equivalent of **1c**.

conformers of **1b**, **1c** and **1c** × $6H^+$ with the use of molecular dynamics at MM level; (ii) full structure optimization at the PCM/PBE0/3-21G* level of conformers found by MD; (iii) frequency analysis at the PCM/PBE0/3-21G* level to confirm the stability of the conformers; (iv) re-optimization of conformer structures with relative energies in the range 0–3 kcal mol^{-1} at the PCM/PBE0/6-31G* level; (v) calculation of the populations of the low-energy conformers of **1b**, **1c** and **1c** × $6H^+$ with relative energies in the range 0.0–2.0 kcal mol^{-1} at the PCM/PBE0/6-31G* level, using Boltzmann statistics and T = 298 K; (vi) calculations of ECD spectra for all low-energy conformers at the PCM/TD-B2LYP level; (vii) Boltzmann averaging of the calculated ECD spectra. The relative energies, populations and some structure determining factors for all $\Delta E_{PBE0/6\text{-}31G*}$ calculated low-energy conformers of **1b**, **1c** and **1c** × $6H^+$ are summarized in Table 2, whereas the structures of the lowest-energy conformers, experimental and calculated ECD spectra of **1b**, **1c** and **1c** × $6H^+$ are shown in Figs 8 and 9.

Previously, we proposed a rational approach for the analysis of trianglamine conformation. In the simplest form, only the rotation about the carbon–nitrogen bonds forming the macrocycle needs to be considered to define the heteraphane conformation. This includes three sets of torsion angles α, α', β, β' for each trianglamine, defined as follows: α (α') = C(N)–C(N)–N(H)–C(HR) and β (β') = C(N)–N–C(HR)–C(Ar). In the case of **1a**, the combination of torsion angles α and β is restricted to either a *gauche* (G^-) or a *trans* (T) arrangement, as confirmed by X-ray data.[16] In the case of **1b**, at least one pair of torsion angles α and β can adopt an *anticlinal* (A^+) conformation, conformers **1b**(1)–**1b**(3). The number of A^+ is limited to three, as each A^+ torsion angle adds to the macrocycle folding and significantly increases its energy (conformers 4 and 5), the third A^+ being separated from the other two by a T-arranged angle, α'. Bulky substituents, such as the phenyl groups, force a more extended conformation of the macrocycle ring to occur. For **1c**, all of the calculated low-energy conformers are characterized by an *all-T* arrangement of torsion angles α and β.

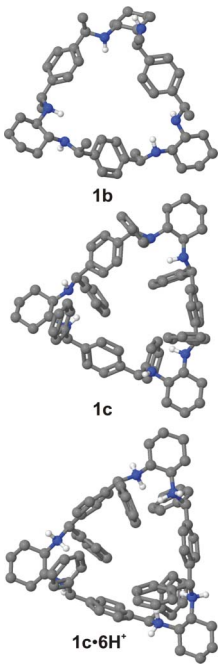

Fig. 8 The structures of the lowest-energy conformers of **1b**, **1c** and **1c** × $6H^+$ calculated at the PCM/PBE0/6-31G* level (some hydrogen atoms are omitted for clarity).

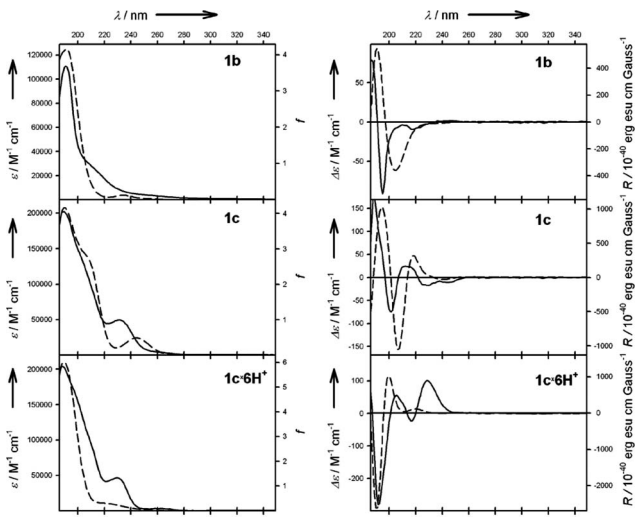

Fig. 9 UV (left panel) and ECD (right panel) spectra for trianglamines **1b**, **1c** and **1c** × $6H^+$ measured in acetonitrile solutions (solid lines) and calculated with the use of PCM/TD DFT method and Boltzmann averaged (dashed lines). Wavelengths have been corrected to match the experimental short-wavelength UV band.

Contrary to **1b**, the relative energy differences between conformers of **1c** are not significant (see Table 2). In the lowest energy conformer, two phenylene rings are in the average macrocycle plane, whereas the third is oriented perpendicularly. Another striking feature of the low-energy conformers of **1c** are the attractive π–π interactions between phenyl substituents. In the case of the lowest-energy conformer (1), three of the six phenyl rings lie much closer and form the "lower" rim of the macrocycle, with calculated distances between the midpoints of phenyl rings of 5.8–6.5 Å. The "upper" rim phenyl rings are at a distance of 8.4–9.2 Å.

Table 2 Relative energies (ΔE, in kcal mol^{-1}), percentage populations and sequences of torsion angles calculated at the PCM/PBE0/6-31G* level for the low-energy conformers of trianglamines **1b**, **1c** and **1c** × 6H$^+$ and predicted signs of ^1B_a exciton Cotton effects generated by each pair of 1,4-disubstituted benzene chromophores

Conformer[a]	ΔE (kcal mol^{-1})	Population (%)	Sequences of torsion angles $\beta\alpha\alpha'\beta'$	Sign of exciton Cotton effect
1b(1)	0.00	55	TTA^+A^+	positive
			$TTTT$	negative
			$TTTT$	negative
1b(2)	0.35	30	$TTTT$	negative
			TTA^+A^+	positive
			$TTTT$	negative
1b(3)	0.96	11	$TTTT$	negative
			TTA^+A^+	positive
			$TTTT$	negative
1b(4)	1.98	2	$TTTT$	negative
			$A^+A^+TA^+$	negative
			$TTTT$	negative
1b(5)	2.00	2	$TTTT$	negative
			$TTTT$	negative
			$A^+A^+TA^+$	negative
1c(1)	0.00	33	$TTTT$	negative
			$TTTT$	negative
			$TTTT$	negative
1c(2)	0.10	29	$TTTT$	negative
			$TTTT$	negative
			$TTTT$	negative
1c(3)	0.59	12	$TTTT$	negative
			$TTTT$	negative
			$TTTT$	negative
1c(4)	0.63	11	$TTTT$	negative
			$TTTT$	negative
			$TTTT$	negative
1c(5)	0.64	11	$TTTT$	negative
			$TTTT$	negative
			$TTTT$	negative
1c(6)	1.20	4	$TTTT$	negative
			$TTTT$	negative
			$TTTT$	negative
1c × 6H$^+$	—	~ 100	TA^+A^+T	negative
			TA^+A^+T	negative
			TA^+A^+T	negative

[a] Conformers are numbered according to their increasing energy.

This arrangement of phenyl substituents makes a hydrophobic pocket where small molecules may be accommodated.

The presence of the dominant conformers of **1b** and **1c** in solution can be determined by ECD spectroscopy. In the case of **1b**, the diagnostic Cotton effects in the CD spectra are due to the ^1B_a type transitions in 1,4-disubstituted benzene chromophores. This transition is polarized along the longitudinal chromophore axis and generates strong exciton Cotton effects with signs and magnitudes depending on the sequences of torsion angles α, α', β, β'. A negative CD contribution is expected due to the *all-T* arrangement of torsion angles α, α', β, β', whereas for the A^+A^+TT sequence the contribution is positive and again negative for the $A^+A^+TA^+$ arrangement of torsion angles α, α', β, β' (see Table 2). Due to the overwhelming domination of *T*-type torsion angles α, α', β, β' in the low-energy conformers of **1b**, the sign of the exciton Cotton couplet is expected to be negative, in good agreement with the experimental data (Fig. 9). A negative CD couplet ($A = -169$) within the strong ^1B_a absorption band at 191 nm ($\varepsilon = 110\,800$) is recorded for **1b** in acetonitrile solution. The ECD spectra calculated for each low-energy conformer of **1b** also show negative exciton Cotton effects (see ESI†), as does the resulting Boltzmann averaged ECD spectrum.

The case of **1c** is more complex, due to the presence of nine aromatic chromophores. The observed short wavelength Cotton effects appear at 201 nm ($\Delta\varepsilon = -75$) and 188 nm ($\Delta\varepsilon = 177$) and form a strong exciton couplet ($A = -252$) related to the strong absorption at 189 nm ($\varepsilon = 202\,400$). The calculated and Boltzmann averaged ECD spectra for the low-energy conformers of **1c** are in good agreement with the experimental data and confirm the postulated structures with *all-T* torsion angles α, α', β and β'. Additional calculations were carried out for a model molecule, constituting one third of real macrocycle **1c** (Fig. 10), which provide support for these structural hypotheses.

The conformation of hexaprotonated derivative **1c** × 6H$^+$ is of special interest, as its ^1B_a exciton Cotton effect is positive, *i.e.* of the opposite sign to **1c** (Fig. 9). Contrary to the non-protonated molecule, characterized by multiple conformational minima, conformational analysis and structure optimization carried out for **1c** × 6H$^+$ led to only one conformer of C_3-symmetry and an unexpected TA^+A^+T sequence of torsion angles α, α', β and β'. The calculated distances between the midpoints of the phenyl rings are 6.7 and 6.9 Å, respectively, for the "lower" and "upper" rims of the macrocycle, and they are shorter than the respective distances (7.6 Å) calculated for the midpoints of 1,4-disubstituted

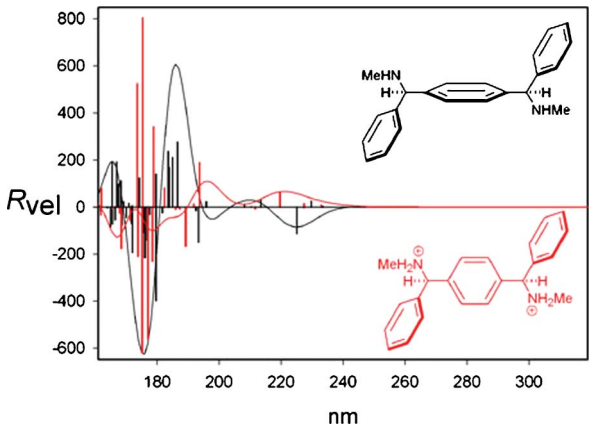

Fig. 10 ECD spectra calculated for model compounds constituting one third of macrocycle **1c** (black) and fully protonated **1c** (red) at the PCM/B2LYP/def2-TZVP level. Wavelengths have not been corrected.

benzenes. An additional structural feature that characterizes the conformation of **1c** × $6H^+$ is the perpendicular orientation of the 1,4-disubstituted benzene rings in relation to the average plane of the macrocycle.

The calculated ECD spectrum of **1c** × $6H^+$ (Fig. 9) is in good agreement with the experimental one, although the magnitude of the calculated long wavelength Cotton effect is underestimated. Note that the sign of the short wavelength exciton couplet due to ^1B_a transitions, predicted from the empirical analysis of the spatial arrangement of 1,4-disubstituted benzene chromophores should be negative, conflicting with the experimental data. This suggests that the ECD spectrum is strongly affected by the interaction of the electronic transitions of the phenyl substituents and less by the interactions between the 1,4-disubstituted benzenes. This hypothesis was confirmed by the analysis of the chiroptical properties of the above mentioned model compound, *i.e.* one-third of **1c** × $6H^+$ (see Fig. 10). It seems reasonable to assume that **1c** × $2H^+$ molecules resulting from adding two carboxylic acid molecules to **1c** are protonated at the nitrogen atoms attached to two different cyclohexane rings and the conformation of the trianglamine macrocycle is *all-T*.

Conclusions

In conclusion, we have tested the applicability of the chiral perazamacrocyclic compound **1c** as a CSA for carboxylic acids, with excellent results. The optimal ratio between **1c** and the racemic acid for a baseline separation of the enantiomers' signals depends on the type of acid, in particular on its degree of acidity: the stronger the acid, the lower the ratios required; the weaker the acid, the higher the ratios needed.

By comparison with the unsubstituted macrocycle **1a**, the introduction of the phenyl substituents in the benzylic positions allows to use a lower amount of the CSA for observing good enantiodiscrimination. The analyte and the CSA could be separated and recovered by a simple acid–base extraction and reused without any purification. ECD spectroscopy combined with DFT calculations was applied to get an insight into the conformations of free and protonated hexaamino macrocycles.

Experimental section

NMR spectra were recorded on a Varian MR 400 (400 MHz) instrument at 25 °C using $CDCl_3$ as a solvent purchased from Sigma–Aldrich. Chemical shifts are reported in ppm relative to the solvent residual peak of $CDCl_3$ (δ_H = 7.27). Spectral assignments were obtained by analysis of chemical shifts and interpretation of ^1H, ^{13}C, gradient COSY, adiabatic gradient HSQC, adiabatic gradient HMBC NMR spectra for a 1 : 2 solution of **1c** and racemic **3a** in $CDCl_3$.[20]

Compounds **3a–f**, **4**, **5**, **7** were purchased from Sigma–Aldrich. Compounds **1b**,[18] **1c**[18] and **6**[23] were prepared according to the literature procedure.

UV and ECD spectra were recorded in acetonitrile solutions with a Jasco J-810 dichrograph.

Computational details

Preliminary conformational searches for all investigated trianglamines were carried out with the use of molecular dynamics, as implemented with CAChe software.[24] Low-energy structures in a trajectory map were the starting points for a geometry optimization at PBE0/3-21G* level using the polarizable continuum model (PCM)[25] for the acetonitrile solution.[26] The structures thus obtained were real minimum energy conformers (no imaginary frequencies have been found). All of the stable conformers were further reoptimized with the use of the same PBE0 density functional 6-31G(d) basis sets and PCM model. ΔE PCM/PBE0/6-31G(d) energy values were used to obtain the Boltzmann population of conformers at 298.15 K. For DFT calculations, only the results for conformers that differ from the most stable by less than 2 kcal mol^{-1} have been taken into account for further calculations, following a generally accepted protocol.[27] For all of the investigated compounds, the ECD spectra were measured in acetonitrile solution and calculated at the PCM/TDDFT/B2LYP/def2-TZVP (trianglamine **1b**) and PCM/TDDFT/B2LYP/def2-SVP (free and protonated **1c**) levels for all stable geometries optimised at the (PCM)/PBE0/6-31G(d) level.[28] Rotatory strengths were calculated using both length and velocity representations. In the present study, the differences between the length and velocity of the calculated values of rotatory strengths were small and for this reason, only the velocity representations were further used. The CD spectra were simulated by overlapping Gaussian functions[29] for each transition, according to the procedure previously described.[30]

Acknowledgements

This work was carried out in the field of the Prin Project: "Sintesi e stereocontrollo di molecole organiche per lo sviluppo di metodologie innovative". Part of this work was supported by a Grant No. N204 555939 from the Ministry of Science and Higher Education (M.K. and J.G.). All calculations have been performed in the Poznan Supercomputing Center.

Notes and references

1 M. Tsukamoto and H. B. Kagan, *Adv. Synth. Catal.*, 2002, **344**, 453–463.

2 W. H. Pirkle and T. C. Pochapsky, *Chem. Rev.*, 1989, **89**, 347–362; V. Schurig and H.-P. Nowotny, *Angew. Chem., Int. Ed. Engl.*, 1990, **29**, 939–957.

3 M. T. Reetz, M. H. Becker, K. M. Kühling and A. Holzwarth, *Angew. Chem., Int. Ed.*, 1998, **37**, 2647–2650; L. Pu, *Chem. Rev.*, 2004, **104**, 1687–1716; Z.-B. Li, J. Lin and L. Pu, *Angew. Chem., Int. Ed.*, 2005, **44**, 1690–1693; J. F. Folmer-Andersen, V. M. Lynch and E. V. Anslyn, *J. Am. Chem. Soc.*, 2005, **127**, 7986–7987; D. Leung, J. F. Folmer-Andersen, V. M. Lynch and E. V. Anslyn, *J. Am. Chem. Soc.*, 2008, **130**, 12318–12327; S. H. Shabbir, L. A. Joyce, G. M. da Cruz, V. M. Lynch, S. Sorey and E. V. Anslyn, *J. Am. Chem. Soc.*, 2009, **131**, 13125–13131; H.-L. Liu, X.-L. Hou and L. Pu, *Angew. Chem., Int. Ed.*, 2009, **48**, 382–385; S. Nieto, J. M. Dragna and Eric V. Anslyn, *Chem.–Eur. J.*, 2010, **16**, 227–232.

4 For a review see: D. Parker, *Chem. Rev.*, 1991, **91**, 1441–1457; T. J. Wenzel and J. D. Wilcox, *Chirality*, 2003, **15**, 256–270; G. Uccello-Barretta, F. Balzano and P. Salvadori, *Curr. Pharm. Des.*, 2006, **12**, 4023–4045.

5 V. M. Mastranzo, L. Quintero and C. A. d. Parrodi, *Chirality*, 2007, **19**, 503–507; C. Sabot, M. Mosser, C. Antheaume, C. Mioskowski, R. Baati and A. Wagner, *Chem. Commun.*, 2009, 3410–3412; N. V. Orlov and V. P. Ananikov, *Chem. Commun.*, 2010, **46**, 3212–3214.

6 D. Yang, X. Li, Y. F. Fan and D. W. Zhang, *J. Am. Chem. Soc.*, 2005, **127**, 7996–7997; C. Peña, J. González-Sabín, I. Alfonso, F. Rebolledo and V. Gotor, *Tetrahedron: Asymmetry*, 2007, **18**, 1981–1985; C. Peña, J. González-Sabín, I. Alfonso, F. Rebolledo and V. Gotor, *Tetrahedron*, 2008, **64**, 7709–7717.

7 G. Uccello-Barretta, L. Vanni and F. Balzano, *Eur. J. Org. Chem.*, 2009, 860–869; X. Lei, L. Liu, X. Chen, X. Yu, L. Ding and A. Zhang, *Org. Lett.*, 2010, **12**, 2540–2543.

8 J. Liao, X. Sun, X. Cui, K. Yu, J. Zhu and J. Deng, *Chem.–Eur. J.*, 2003, **9**, 2611–2615; M. Ardej-Jakubisiak and R. Kawecki, *Tetrahedron: Asymmetry*, 2008, **19**, 2645–2647; J. Redondo, A. Capdevila and I. Latorre, *Chirality*, 2010, **22**, 472–478.

9 M. Claeys-Bruno, D. Toronto, J. Pécaut, M. Bardet and J.-C. Marchon, *J. Am. Chem. Soc.*, 2001, **123**, 11067–11068; T. Ema, N. Ouchi, T. Doi, T. Korenaga and T. Sakai, *Org. Lett.*, 2005, **7**, 3985–3988.

10 K. A. Provencher, M. A. Weber, L. A. Randall, P. R. Cunningham, C. F. Dignam and T. J. Wenzel, *Chirality*, 2010, **22**, 336–346; E. Rudzińska, G. Dziędziołа, L. Berlicki and P. Kafarski, *Chirality*, 2010, **22**, 63–68.

11 T. J. Wenzel, J. E. Thurston, D. C. Sek and J.-P. Joly, *Tetrahedron: Asymmetry*, 2001, **12**, 1125–1130; G. Heinrichs, L. Vial, J. Lacour and S. Kubik, *Chem. Commun.*, 2003, 1252–1253; X. M. Yang, X. J. Wu, M. H. Fang, Q. Yuan and E. Q. Fu, *Tetrahedron: Asymmetry*, 2004, **15**, 2491–2497; Y.-S. Zheng and C. Zhang, *Org. Lett.*, 2004, **6**, 1189–1192; C. F. Dignam, C. J. Richards, J. J. Zopf, L. S. Wacker and T. J. Wenzel, *Org. Lett.*, 2005, **7**, 1773–1776; G. Uccello-Barretta, F. Balzano, J. Martinelli, M.-G. Berni, C. Villani and F. Gasparrini, *Tetrahedron: Asymmetry*, 2005, **16**, 3746–3751; Y. Nakatsuji, Y. Nakahara, A. Muramatsu, T. Kida and M. Akashi, *Tetrahedron Lett.*, 2005, **46**, 4331–4335; X. X. Liu and Y. S. Zheng, *Tetrahedron Lett.*, 2006, **47**, 6357–6360; F. N. Ma, L. Ai, X. M. Shen and C. Zhang, *Org. Lett.*, 2007, **9**, 125–127; A. E. Lovely and T. J. Wenzel, *Chirality*, 2008, **20**, 370–378; T. Ema, D. Tanida, K. Hamada and T. Sakai, *J. Org. Chem.*, 2008, **73**, 9129–9132.

12 For a review on chiral perazamacrocycles, see: D. Savoia and A. Gualandi, *Curr. Org. Synth.*, 2009, **6**, 119–142; D. Savoia and A. Gualandi, *Curr. Org. Synth.*, 2009, **6**, 102–118.

13 For a review on chiral molecular receptors based on *trans*-1,2-diaminocyclohexane, see: I. Alfonso, *Curr. Org. Synth.*, 2010, **7**, 1–23.

14 A. González-Álvarez, I. Alfonso and V. Gotor, *Tetrahedron Lett.*, 2006, **47**, 6397–6400; E. Busto, A. González-Álvarez, V. Gotor-Fernández, I. Alfonso and V. Gotor, *Tetrahedron*, 2010, **66**, 6070–6077.

15 K. Tanaka, N. Fukuda and T. Fujiwara, *Tetrahedron: Asymmetry*, 2007, **18**, 2657–2661.

16 J. Gawronski, H. Kolbon, M. Kwit and A. Katrusiak, *J. Org. Chem.*, 2000, **65**, 5768–5773; J. Gawronski, K. Gawronska, J. Grajewski, M. Kwit, A. Plutecka and U. Rychlewska, *Chem.–Eur. J.*, 2006, **12**, 1807–1817.

17 K. Tanaka and N. Fukuda, *Tetrahedron: Asymmetry*, 2009, **20**, 111–114.

18 D. Savoia, A. Gualandi and H. Stoeckli-Evans, *Org. Biomol. Chem.*, 2010, **8**, 3992–3996.

19 M. Periasamy, M. Dalai and M. Padmaja, *J. Chem. Sci.*, 2010, **122**, 561–569.

20 See electronic supporting information†.

21 P. Job, *Ann. Chim.*, 1928, **9**, 113–203; P. Job, *C. R. Hebd. Seances Acad. Sci.*, 1925, **180**, 928–930; M. T. Blanda, J. H. Horner and M. Newcomb, *J. Org. Chem.*, 1989, **54**, 4626–4636.

22 F. Ma, X. Shen, X. Ming, J. Wang, J. Ou-Yang and C. Zhang, *Tetrahedron: Asymmetry*, 2008, **19**, 1576–1586.

23 L. Gentilucci, L. Cerisoli, R. D. Marco and A. Tolomelli, *Tetrahedron Lett.*, 2010, **51**, 2576–2579.

24 CAChe WS Pro 5.0 Fujitsu Ltd.

25 B. Mennucci, J. Tomasi, R. Cammi, J. R. Cheeseman, M. Frisch, F. J. Devlin, S. Gabriel and P. J. Stephens, *J. Phys. Chem.*, 2002, **106**, 6102–6113; D. Marchesan, S. Coriani, C. Forzato, P. Nitti, G. Pitacco and K. Ruud, *J. Phys. Chem. A*, 2005, **109**, 1449–1453; G. Scalmani, M. J. Frisch, B. Mennucci, J. Tomasi, R. Cammi and V. Barone, *J. Chem. Phys.*, 2006, **124**, 094107.

26 *Gaussian 03 (Revision D.0)*, M. A. Robb, J. R. Cheeseman, J. A. Montgomery, Jr., T. Vreven, K. N. Kudin, J. C. Burant, J. M. Millam, S. S. Iyengar, J. Tomasi, V. Barone, B. Mennucci, M. Cossi, G. Scalmani, N. Rega, G. A. Petersson, H. Nakatsuji, M. Hada, M. Ehara, K. Toyota, R. Fukuda, J. Hasegawa, M. Ishida, T. Nakajima, Y. Honda, O. Kitao, H. Nakai, M. Klene, X. Li, J. E. Knox, H. P. Hratchian, J. B. Cross, V. Bakken, C. Adamo, J. Jaramillo, R. Gomperts, R. E. Stratmann, O. Yazyev, A. J. Austin, R. Cammi, C. Pomelli, J. W. Ochterski, P. Y. Ayala, K. Morokuma, G. A. Voth, P. Salvador, J. J. Dannenberg, V. G. Zakrzewski, S. Dapprich, A. D. Daniels, M. C. Strain, O. Farkas, D. K. Malick, A. D. Rabuck, K. Raghavachari, J. B. Foresman, J. V. Ortiz, Q. Cui, A. G. Baboul, S. Clifford, J. Cioslowski, B. B. Stefanov, G. Liu, A. Liashenko, P. Piskorz, I. Komaromi, R. L. Martin, D. J. Fox, T. Keith, M. A. Al-Laham, C. Y. Peng, A. Nanayakkara, M. Challacombe, P. M. W. Gill, B. Johnson, W. Chen, M. W. Wong, C. Gonzalez and J. A. Pople, Gaussian, Inc., Wallingford CT, 2004.

27 P. J. Stephens, D. M. McCann, E. Butkus, S. Stončius, J. R. Cheeseman and M. J. Frisch, *J. Org. Chem.*, 2004, **69**, 1948–1958; P. J. Stephens, F. J. Devlin, J. R. Cheeseman, M. J. Frisch, O. Bortolini and P. Besse, *Chirality*, 2003, **15**, S57–S64.

28 Ahlrichs, M. Baer, M. Haeser, H. Horn and C. Koelmel, *Chem. Phys. Lett.*, 1989, **162**, 165–169 (see also www.turbomole-gmbh.com for an overview of the TURBOMOLE program); S. Grimme, *J. Chem. Phys.*, 2006, **124**, 034108; S. Grimme and F. Neese, *J. Chem. Phys.*, 2007, **127**, 154116; L. Goerigk and S. Grimme, *J. Phys. Chem. A*, 2009, **113**, 767–776; J. Gawronski, M. Kwit and P. Skowronek, *Org. Biomol. Chem.*, 2009, **7**, 1562–1572.

29 N. Harada and P. Stephens, *Chirality*, 2010, **22**, 229–233; N. M. O'Boyle, A. L. Tenderholt and K. M. Langner, *J. Comput. Chem.*, 2008, **29**, 839–845.

30 D. R. Boyd, A. Drake, J. Gawronski, M. Kwit, J. F. Malone and N. D. Sharma, *J. Am. Chem. Soc.*, 2005, **127**, 4308–4319.